Spark plasma sintering of α/β-SiAlON synthesized by salt-assisted combustion

Jing Niu[a], *Xuemei Yi*[a,b], *Kazuto Harada*[c], *Tomohiro Akiyama*[a #]

[a]*Center for Advanced Research of Energy and Materials, Hokkaido University, Kita 13 Nishi 8, Kitaku, Sapporo 060-8628, Japan.*

[b]*College of Mechanical and Electronic Engineering, Northwest A&F University, Xinong Road 22, Yangling, Shaanxi 712100, China*

[c]*Combustion Synthesis Co. Ltd., Numazu, Shizuoka 410-0801, Japan.*

[#]Corresponding author: Tel: +81 11 706 6842; Fax: +81 11 726 0731

E-mail address: takiyama@eng.hokudai.ac.jp

Abstract

This paper describes the spark plasma sintering (SPS) of Y- and Ca-α/β-SiAlON powders synthesized by salt-assisted combustion at temperatures of 1600 °C with different holding times. X-ray diffraction reveals that with increasing holding time, the α to β transformation ratio of Y-α-SiAlON becomes greater than that of Ca-α-SiAlON. Nevertheless, all samples effectively reach their theoretical density after sintering. The Vickers hardness measured with an applied load of 19.614 (2.0 kg) decreases with a decreasing amount of α-SiAlON, with a maximum value of 19.4 GPa being achieved in Ca-α/β-SiAlON with an α-SiAlON content of 55%.

Keywords: SiAlON; Salt-assisted synthesis; Spark plasma sintering; Phase transformation; Vickers hardness.

1. Introduction

Ceramics produced from SiAlON typically have one of two structures depending on their general chemical formula. The first of these is α-SiAlON, which has a formula of $M_x^vSi_{12-(m+n)}Al_{m+n}O_nN_{16-n}$ ($x = m/v$; v is the valence of the metal, and M represents Li, Mg, Ca, Y, or a rare earth metal) and generally exhibits equiaxed grains. The other is β-SiAlON, or $Si_{6-z}Al_zO_zN_{8-z}$ (where z denotes the number of Si–N bonds substituted by the Al–O bonds ($0 < z \leq 4.2$) [1-3]), which forms elongated grains. These differences mean that although α-SiAlON has a higher Vickers hardness and resistance to oxidation and erosion, β-SiAlON has greater strength and toughness. In recent years, this has led to increased interest in mixed α/β-SiAlON materials as a means of providing superior mechanical properties in pure α-SiAlON, as well as any α-SiAlON composites or polytypes [4-6].

Methods that have been used to produce α/β-SiAlON or α-SiAlON ceramics include hot-pressing (HP) [6], pressure-less sintering [7], reaction sintering [8], carbothermal reduction and nitridation (CRN) [9], and combustion synthesis (CS) [10-13]. Among these, combustion synthesis (CS) has proven to be particularly effective in terms of energy- and time-savings due to the simplicity of the equipment needed, short reaction time and high-purity product obtained. However, spark plasma

sintering (SPS) has recently emerged as a rapid and effective technique for densifying ceramics and composites at relatively low temperatures and with short holding times compared to conventional techniques. In addition, SPS provides high heating rates that increase the possibility of obtaining fine-grained products [14-16].

In previous studies, we successfully synthesized high purity β-SiAlON and α/β-SiAlON powders by adding a small amount of NaCl or $MgCl_2$ to the reaction mixture for salt-assisted combustion synthesis instead of traditional SiAlON diluents [12,17]. These diluents were selected on the basis of their high latent and sensible heat; however, it was unclear the products synthesized by this new method could be sintered to form a dense product. The present work therefore aims to densify SiAlON powders fabricated by salt-assisted combustion synthesis using relatively low temperature (1600 °C) SPS. The effect of varying the holding time of this process on the α/β-SiAlON phase composition, microstructure and Vickers hardness of the final specimen is also explored.

2. Experimental procedure

The starting materials used for this study were Si (purity >99.9%, 12 μm), Al (purity >99.9%, 14 μm), CaO (purity >99.9%), and Y_2O_3 (purity >99.9%) powders,

with NaCl (purity >99.9%) and $MgCl_2$ (purity >99.9%) being used as diluents. The raw powders were mechanically activated by planetary ball-milling at a ball-to-sample mass ratio of 10:1 for 15 min. Si_3N_4 balls with the diameter of ϕ 5 mm were used, and the rotation speed was fixed at 300 rpm. Next, 120 g of the activated mixture was loosely packed into a graphite crucible with dimensions 80 ×130 × 45 mm, which after removing any air, was charged with 1 MPa of nitrogen (purity: 99.99%). Combustion was triggered by igniting an igniter agent of 3 g Al and β-SiAlON mixtures (Al/β-SiAlON = 50/50 mass%) by passing an electric current through carbon foil placed on one end of the raw sample. A detailed description of the experimental setup used for combustion synthesis can be found in previous reports [18]. Using this method, two different compositions of α/β-SiAlON were fabricated with chemical formulae of $Y_{0.2}Si_{11.1}Al_{0.9}O_{0.3}N_{15.7}$ (m = 0.6, n = 0.3) and $Ca_{0.3}Si_{11.1}Al_{0.9}O_{0.3}N_{15.7}$ (m = 0.6, n = 0.3). The compositions and names given to these samples are listed in Table 1.

After cooling, the synthesized products were crushed and washed several times with distilled water to remove any remaining salts, and were then dried at 70 °C for 24 h. The dry powders were subsequently planetary milled in absolute ethyl alcohol using Al_2O_3 balls in a plastic jar until an average particle size of about 0.5 μm was achieved (as determined by a laser light scattering, Horiba, Japan). The resulting slurry was dried

at 70 °C for 24 h, and then compacted into a carbon die with a 10 mm inner diameter and sintered using a SPS system under a vacuum of lower than 6 Pa at a compressive stress of 50 MPa. The sample temperature was monitored by using an optical pyrometer, focused on a hole on the surface of the carbon die. The compacts were heated from room temperature to 600 °C over a period of 5 min, and then heated to 1600 °C at a rate of 30 °C /min with holding times varying from 0 to 10 min. A flowchart of the experimental procedure is shown in Fig. 1.

The phases of the products were analyzed using X-ray diffraction (XRD, Miniflex, Rigaku, Japan) with Cu Kα radiation (λ = 1.54056 nm). Polished surfaces of the sintered samples were examined by SEM after carbon coating using a back scattered electron imaging mode (FE-SEM, JSM-7400F, JEOL, Japan). The amount of α- and β-SiAlON present was estimated by comparing the intensities of the strongest XRD peaks for these two phases, which are the (210) peaks of both α- and β-SiAlON [19]. The bulk densities of the sintered specimens were measured according to Archimedes' principle. Vickers hardness testing was carried out at room temperature using a diamond indenter with an indentation load of 2 kgf (9.81 N) for 20 s. At least 5 indentations were made for each sample.

3. Results and discussion

In previous work, 12 mass% NaCl and 18 mass% $MgCl_2$ addition was needed to achieve complete nitridation of Si in the salt-assisted combustion synthesis of α/β-SiAlON [12]. Based on this, the same amounts of NaCl and $MgCl_2$ were added to the reactant powders in the present study. The XRD patterns of the as-synthesized samples in Fig. 2 show α- and β-SiAlON crystalline phases present in all samples, with the very small amount of unreacted Si indicating that nitridation was achieved. A qualitative estimate of the relative amounts of α- and β-phase in these samples was performed using the relative intensities of the (210) reflections for both α- and β-SiAlON. The Ca0.3N12 and Y0.2N12 samples obtained by adding 12 mass% NaCl had a relatively greater weight fraction of α-phase SiAlON (94% and 76%, respectively). In contrast, the Ca0.3M18 and Y0.2M18 samples obtained with the addition of 18 mass% $MgCl_2$ exhibit much lower α-phase SiAlON contents of 7% and 56%. These results are consistent with our previous work, which showed that NaCl is more efficient at promoting the formation of α-phase SiAlON [12]. It should be noted, however, that these values are only approximate, as any amorphous phase fractions cannot be determined precisely using this method.

Figure 3 shows the densification behavior of Y- and Ca-α-SiAlON sintered at

1600 °C with 10 min holding time. The decreased displacement evident during the initial sintering stage can be attributed to the thermal expansion of the sample powders and carbon die. When the sintering temperature exceeded 1300 °C, densification started and quickly proceeded to a peak value within approximately 10 min. No further change was observed after this time, which suggests that near-complete dense products can be obtained even without holding at the final sintering temperature.

The XRD patterns of the Y0.2N12 sample after sintering at 1600 °C with different holding times (Fig. 4) show that the initial trace amount of Si disappears through either vaporization or dissolution into the solid during sintering [20]. Furthermore, the 50 mass% of α-SiAlON when sintered without holding is completely transformed to β-phase SiAlON after a 3-min holding time. This indicates that α-β transformation can occur during sintering at 1600 °C, and that the amount of α-SiAlON decreases with increasing holding time.

With the Ca0.3N12 sample sintered at 1600 °C with different holding times, the XRD patterns in Fig. 5 show that approximately 8 mass% of the α-phase remains even after a 10-min holding time. This indicates that the fraction of β-phase SiAlON increases with holding time, and that the α to β transformation ratio is lower for Ca-α-SiAlON than for Y-α-SiAlON. Some reports have shown that in the Ca-SiAlON

system, Ca-α-SiAlON not only has a much larger stability field than rare earth α-SiAlON, but is also much more resistant to α-β transformation. This distinction is due to the lower valency of Ca (2+), as α-SiAlON stability increases with increasing cation solubility x (where x=m/v, and v is the cation valency), which in turn increases with decreasing cation valency [21-23].

In the XRD patterns of the Y0.2M18 and Ca0.3M18 samples sintered at 1600 °C shown in Fig. 6, no α-phase SiAlON was observed regardless whether there was a holding time or not. This means that complete α-β transformation occurred due to the lower amount of α-SiAlON that was contained in these samples prior to sintering.

A number of back-scattered scanning electron micrographs were obtained from polished surfaces of the sintered specimens. The micrographs of Y0.2N12 sintered at 1600 °C in Fig. 7 show that without a holding time the sintered product mainly contained α-SiAlON grains (light grey) surrounded by a small amount of grain-boundary glass (white) and β-SiAlON grains (dark grey). With a 3-min holding time, however, the β-SiAlON grains developed into rod-like particles ~3 μm in length and more intergranular phases appeared. These rod-like β-SiAlON particles should exhibit greater fracture toughness than α-SiAlON, but further study is needed to determine their mechanical properties. As no porosity was observed in any of the

sample, it is assumed that they all essentially reached their theoretical maximum density.

Although the back-scattered electron micrographs of Ca0.3N12 sintered at 1600 °C in Fig. 8 show some contrast, it is difficult to differentiate between α and β phases in the same way as the Y-α-SiAlON sample in Fig. 7 due to the lower atomic number of Ca (20). Nevertheless, it appears as if the area of dark β-SiAlON grains increases with holding time (the white dots can be regarded as a glass phase containing Ca). The polished surfaces of these samples exhibited only a few micro-pores, indicating that they too were essentially of theoretical maximum density after SPS at 1600 °C.

Table 2 summarizes the density, phase composition and Vickers hardness of the various samples after sintering under different conditions. It can be seen very clearly from this that the hardness decreases with decreasing α-SiAlON content, which is due to equiaxed α-SiAlON grains transforming into elongated β-SiAlON and precipitating inter-granular phases during sintering. However, as demonstrated by Liu et al. [24], the elongated β-SiAlON grains enhance the fracture toughness. A maximum hardness of 19.4 GPa was achieved with the Ca0.3N12 sample with an α-phase content of 55%, which is higher than has been achieved with pure-phase β-SiAlON or α-SiAlON prepared by a combination of combustion synthesis and SPS [25,26].

4. Conclusions

Investigation of the spark plasma sintering of Y- and Ca-α/β-SiAlON prepared by salt-assisted combustion synthesis has demonstrated that compaction to full density is possible at a relatively low temperature of 1600 °C. The use of NaCl or $MgCl_2$ during synthesis reduces both the financial cost and energy requirements for production. The α to β transformation that occurs during sintering increases with holding time, resulting in a microstructural change from equiaxed α-SiAlON grains to elongated grains of β-SiAlON and grain boundary phases that reduces the Vickers hardness. Nevertheless, a maximum hardness of 19.4 GPa was achieved with Ca-α/β-SiAlON containing 55% α phase that was higher than has been achieved with either phase on its own. As this process makes it possible to control the phase composition and microstructure by varying the SPS parameters, it has the potential to open up new applications for these materials.

Acknowledgements

This work was financially supported by the 2014 Strategic Foundational Technology Improvement Support Operation of the Ministry of Economy, Trade and Industry (No. 24110105008, Development of high-quality and economical SiAlON powders by combustion synthesis method).

References

[1] K.H. Jack, Review: SiAlONs and related nitrogen ceramics, J. Mater. Sci. 11 (1976) 1135-1158.

[2] T. Ekström, P.O. Käll, M. Nygren, P.O. Olssen, Dense single-phase β-SiAlON ceramics by glass-encapsulated hot isostatic pressing, J. Mater. Sci. 24 (1989) 1853-1861.

[3] T. Ekström, M. Nygren, SiAlON ceramics, J. Am. Ceram. Soc. 75[2] (1992) 259-276.

[4] S. Bandyopadhyay, M.J. Hoffmann, G. Petzow, Densification behavior and properties of Y_2O_3-containing α-SiAlON-based composites, J. Am. Ceram. Soc. 79 (1996) 1537-1545.

[5] T.-S. Sheu, Microstructure and mechanical properties of the in situ β-Si_3N_4/α′-SiAlON composite, J. Am. Ceram. Soc. 77 (1994) 2345-2353.

[6] F. Ye, L. Liu, H. Zhang, Y. Zhou, Z. Zhang, Novel mixed α/β-SiAlONs with both elongated α and β grains, Scripta Mater. 60 (2009) 471-474.

[7] Y.-W. Li, P.-L. Wang, W.-W. Chen, Y.-B. Cheng, D.-S. Yan, Phase formation and microstructural evolution of Ca-α-SiAlON using different Si_3N_4 starting powders, J. Eur. Ceram. Soc. 20 (2000) 1803-1808.

[8] J.W.T. van Rutten, H.T. Hintzen, R. Metselaar, Phase formation of Ca-α-SiAlON by reaction sintering, J. Eur. Ceram. Soc. 16 (1996) 995-999.

[9] J. Huang, H. Zhou, Z. Huang, G. Liu, M. Fang, Y.g. Liu, Preparation and formation mechanism of elongated (Ca,Dy)-α-SiAlON powder via carbothermal reduction and nitridation, J. Am. Ceram. Soc. 95 (2012) 1871-1877.

[10] G. Liu, K. Chen, H. Zhou, C. Pereira, J. Ferreira, Novel faceted α-SiAlON micro-crystals prepared by combustion synthesis, J. Am. Ceram. Soc. 89 (2006) 364-366.

[11] G. Liu, K. Chen, H. Zhou, X. Ning, C. Pereira, J.M.F. Ferreira, Fabrication of yttrium-stabilized α-SiAlON powders with rod-like crystals by combustion synthesis, J. Mater. Sci. 41 (2006) 6062-6068.

[12] J. Niu, K. Harada, S. Suzuki, I. Nakatsugawa, N. Okinaka, T. Akiyama, Fabrication of mixed α/β-SiAlON powders via salt-assisted combustion synthesis, J. Alloys. Compd. 604 (2014) 260-265.

[13] C.L. Yeh, F.S. Wu, Y.L. Chen, Effects of α- and β-Si_3N_4 as precursors on combustion synthesis of (α+β)-SiAlON composites, J. Alloys. Compd. 509 (2011) 3985-3990.

[14] D. Salamon, Z. Shen, P. Šajgalík, Rapid formation of α-SiAlON during spark plasma sintering: Its origin and implications, J. Eur. Ceram. Soc. 27 (2007) 2541-2547.

[15] D. Jiang, D.M. Hulbert, J.D. Kuntz, U. Anselmi-Tamburini, A.K. Mukherjee, Spark plasma sintering: A high strain rate low temperature forming tool for ceramics, Mater. Sci. Eng. A 463 (2007) 89-93.

[16] D. Sciti, S. Guicciardi, M. Nygren, Spark plasma sintering and mechanical behaviour of ZrC-based composites, Scripta Mater. 59 (2008) 638-641.

[17] J. Niu, K. Harada, I. Nakatsugawa, T. Akiyama, Morphology control of β-SiAlON via salt-assisted combustion synthesis, Ceram. Inter. 40 (2014) 1815-1820.

[18] J. Niu, T. Nakamura, I. Nakatsugawa, T. Akiyama, Reaction characteristics of combustion synthesis of β-SiAlON using different additives, Chem. Eng. J. 241

(2014) 235-242.

[19] C. P.Gazzara, D.R. Messier, Determination of phase content of Si_3N_4 by X-Ray diffraction analysis, Ceram. Bull. 56 (1977) 777-780.

[20] X. Yi, K. Watanabe, T. Akiyama, Fabrication of dense β-SiAlON by a combination of combustion synthesis (CS) and spark plasma sintering (SPS), Intermetallics 18 (2010) 536-541.

[21] C. L. Hewett, Y. B. Cheng, B. C. Muddle and M. B. Trigg, Thermal stability of calcium α-SiAlON Ceramics, J. Eur. Ceram. Soc. 18 (1998) 417-427.

[22] H. Mandal, D.P. Thompson, α→ β SiAlON transformation in calcium-containing α-SiAlON ceramics, J. Eur. Ceram. Soc. 19 (1999) 543-552.

[23] H. Mandal, New developments in α-SiAlON ceramics, J. Eur. Ceram. Soc. 19 (1999) 2349-2357.

[24] Q. Liu, L. Gao, D. S. Yan, D. P. Thompson, Thermal stability and mechanical performance of multiply heat-treated α-SiAlON ceramics densified with rare earth oxides, J. Mater. Sci. 35 (2000) 2229-2233.

[25] X. Yi, K. Watanabe, T. Akiyama, Vickers hardness of β-SiAlON prepared by a combination of combustion synthesis and spark plasma sinterng, J. Ceram. Soc. Japan 118 (2010) 250-252.

[26] M. Koshiyama, H. Sako, M. Ohno, K. Matsuura, Relationships between spark plasma sintering temperature and mechanical properties of combustion-synthesized α- and β-SiAlON, J. Japan Inst. Met. Mater. 79 (2015) 191-194.

Table 1

Starting compositions of the samples

Sample	Composition (mass%)					
	NaCl	$MgCl_2$	Si	Al	CaO	Y_2O_3
Ca0.3N12	12	0	77.72	6.08	4.20	0
Ca0.3M18	0	18	72.42	5.66	3.91	0
Y0.2N12	12	0	76.46	5.98	0	5.56
Y0.2M18	0	18	71.25	5.57	0	5.18

Table 2

Density, phase composition and Vickers harness of specimens sintered at 1600 ºC with different holding times.

Sample	Holding time (min)	Measured density (g/cm^3)	Phases (mass %)		Vickers hardness (GPa)
			α-SiAlON	β-SiAlON	
Ca0.3N12	0	3.14	61	39	19.4
	3	3.12	29	71	17.5
	10	3.11	10	90	16.2
Y0.2N12	0	3.16	40	60	17.8
	3	3.16	0	100	17.2
	10	3.17	0	100	17.3
Y0.2M18	0	3.16	0	100	16.4
	10	3.16	0	100	15.8
Ca0.3M18	10	3.16	0	100	16.4

Figure captions

Fig. 1 Flow chart of the experimental procedure used.

Fig. 2 XRD patterns of combustion synthesized Ca- and Y-α/β-SiAlON powders with the addition of 12 mass% NaCl (Ca0.3N12, Y0.2N12) and 18 mass% $MgCl_2$ (Ca0.3M18, Y0.2M18).

Fig. 3 Densification curves of Y- and Ca-α-SiAlON sintered at 1600 °C with holding 10 minutes.

Fig. 4 XRD patterns of the Y0.2N12 sintered at 1600 °C with (a) 0 minutes: no holding, (b) 3 minutes and (c) 10 minutes holding time.

Fig. 5 XRD patterns of the Ca0.3N12 sintered at 1600 °C with (a) 0 minutes: no holding, (b) 3 minutes and (c) 10 minutes holding time.

Fig. 6 XRD patterns of the Y0.2M18 and Ca0.3M18 sintered at 1600 °C with different holding time.

Fig. 7 The back-scattered micrographs of polished surfaces of the Y0.2N12 sintered at 1600 °C with (a) 0 minutes: no holding and (b) 3 minutes holding time. α-SiAlON, β-SiAlON, and glass phase have grey, black, and white contrast, respectively.

Fig. 8 The back-scattered micrographs of polished surfaces of the Ca0.3N12 sintered at 1600 °C with (a) 0 minutes: no holding, (b) 3 minutes and (c) 10 minutes holding time.

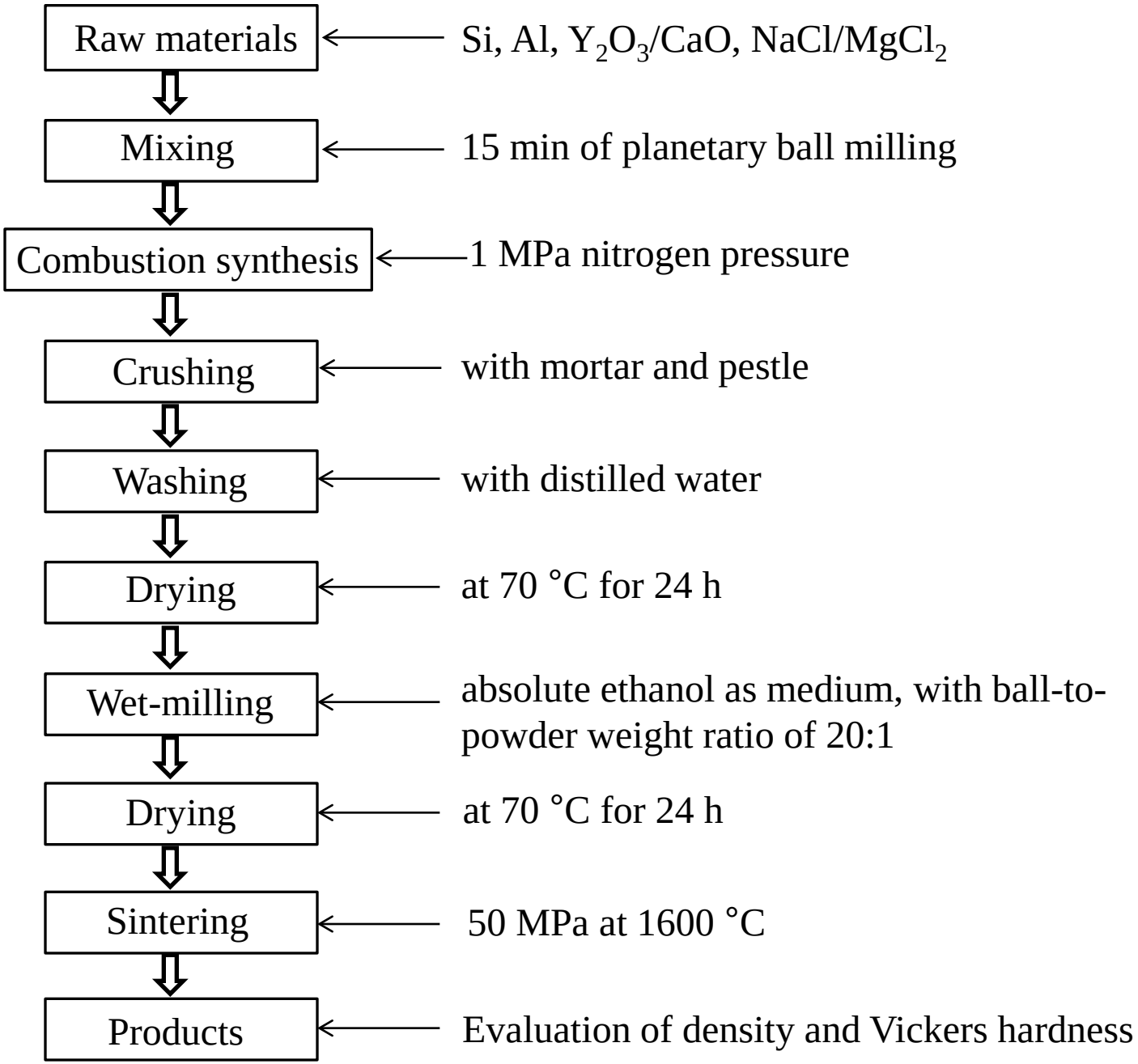

Fig. 1 Flow chart of the experimental procedure used

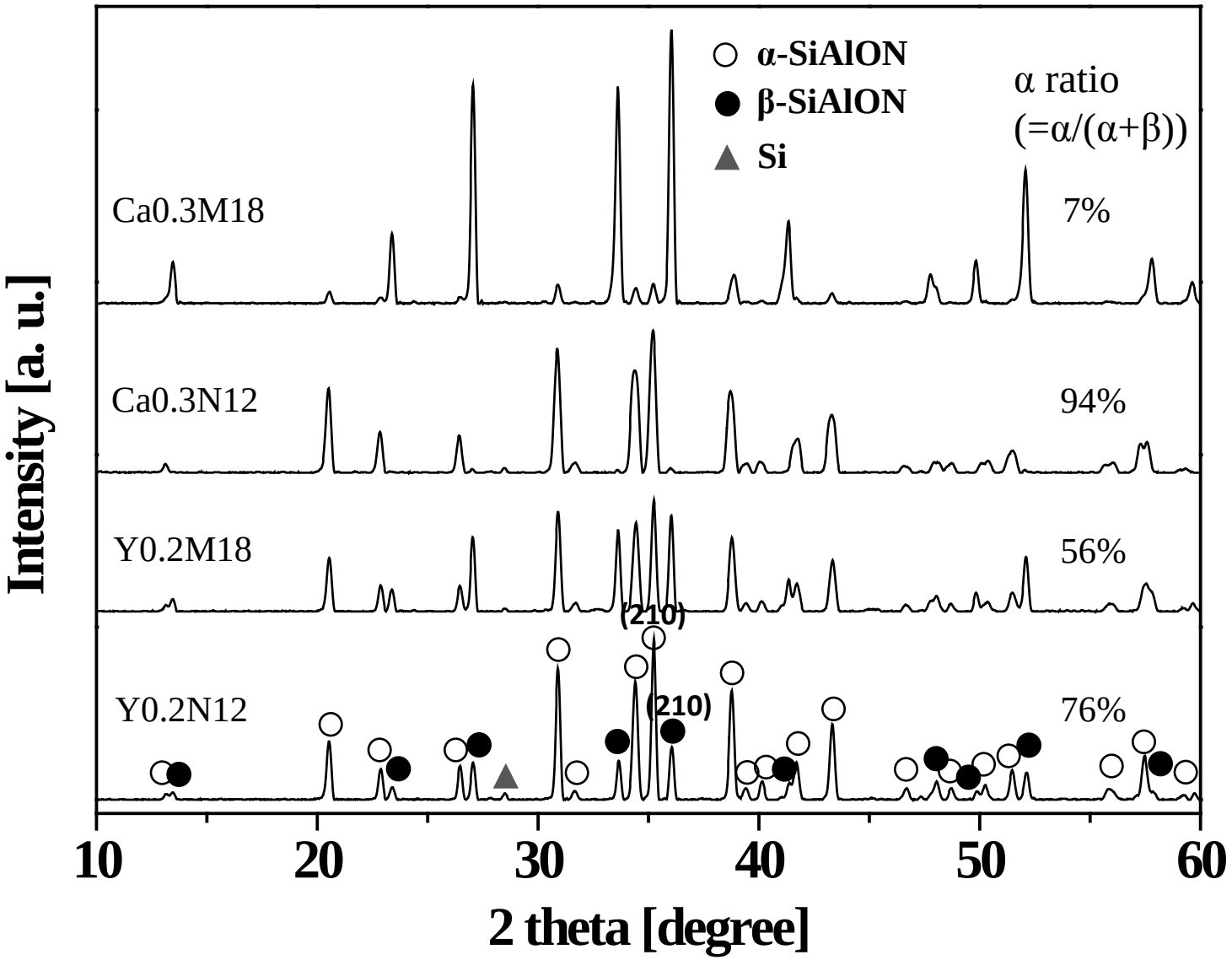

Fig. 2 XRD patterns of combustion synthesized Ca- and Y-α/β-SiAlON powders with 12 mass% NaCl (Ca0.3 N12, Y0.2 N12) and 18 mass% $MgCl_2$ (Ca0.3 M18, Y0.2 M18) addition.

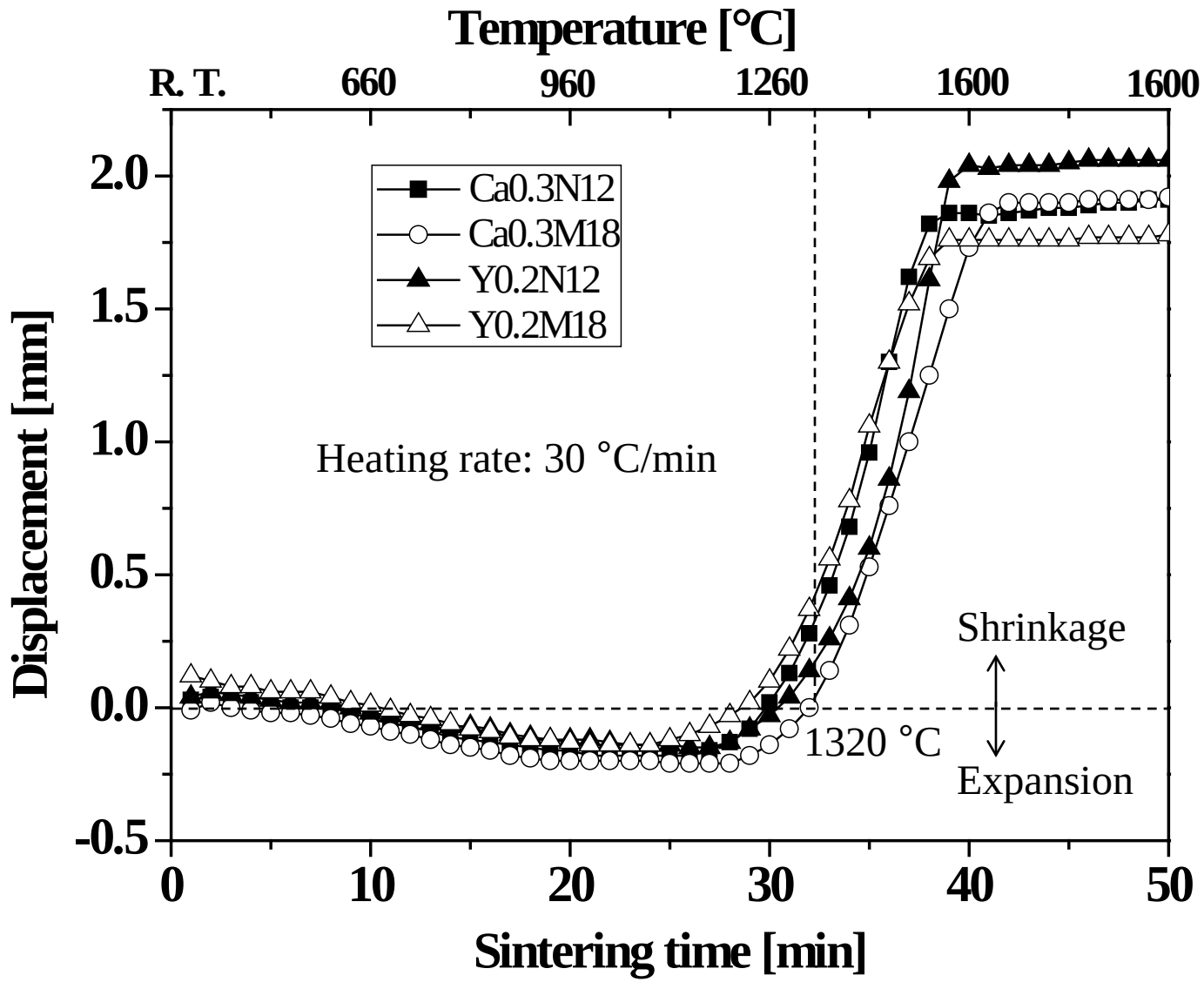

Fig. 3 Densification curves of Y- and Ca-α-SiAlON sintered at 1600 ºC for 10 min.

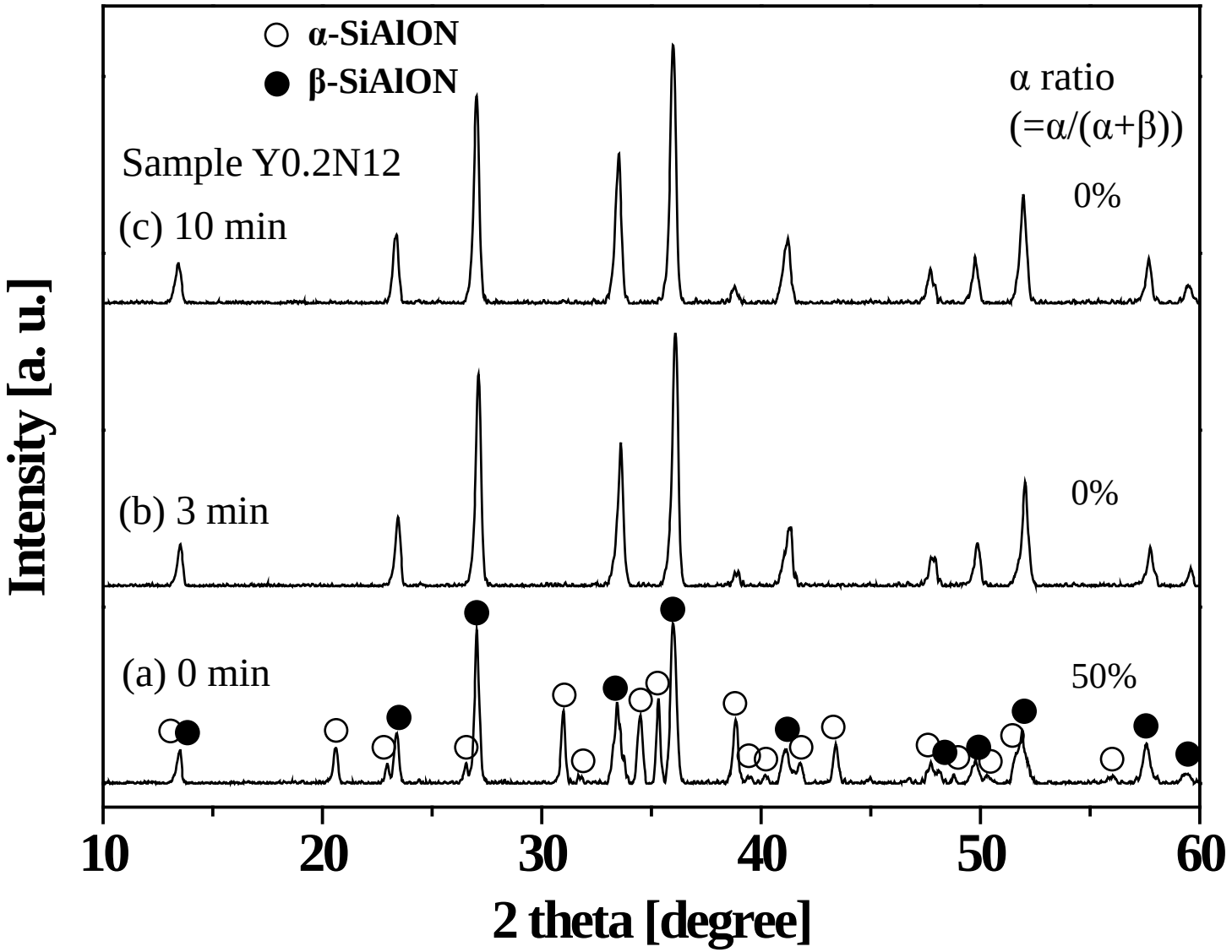

Fig. 4 XRD patterns of Y0.2N12 sintered at 1600 ºC for: (a) 0 min: no holding, (b) 3 min and (c) 10 min.

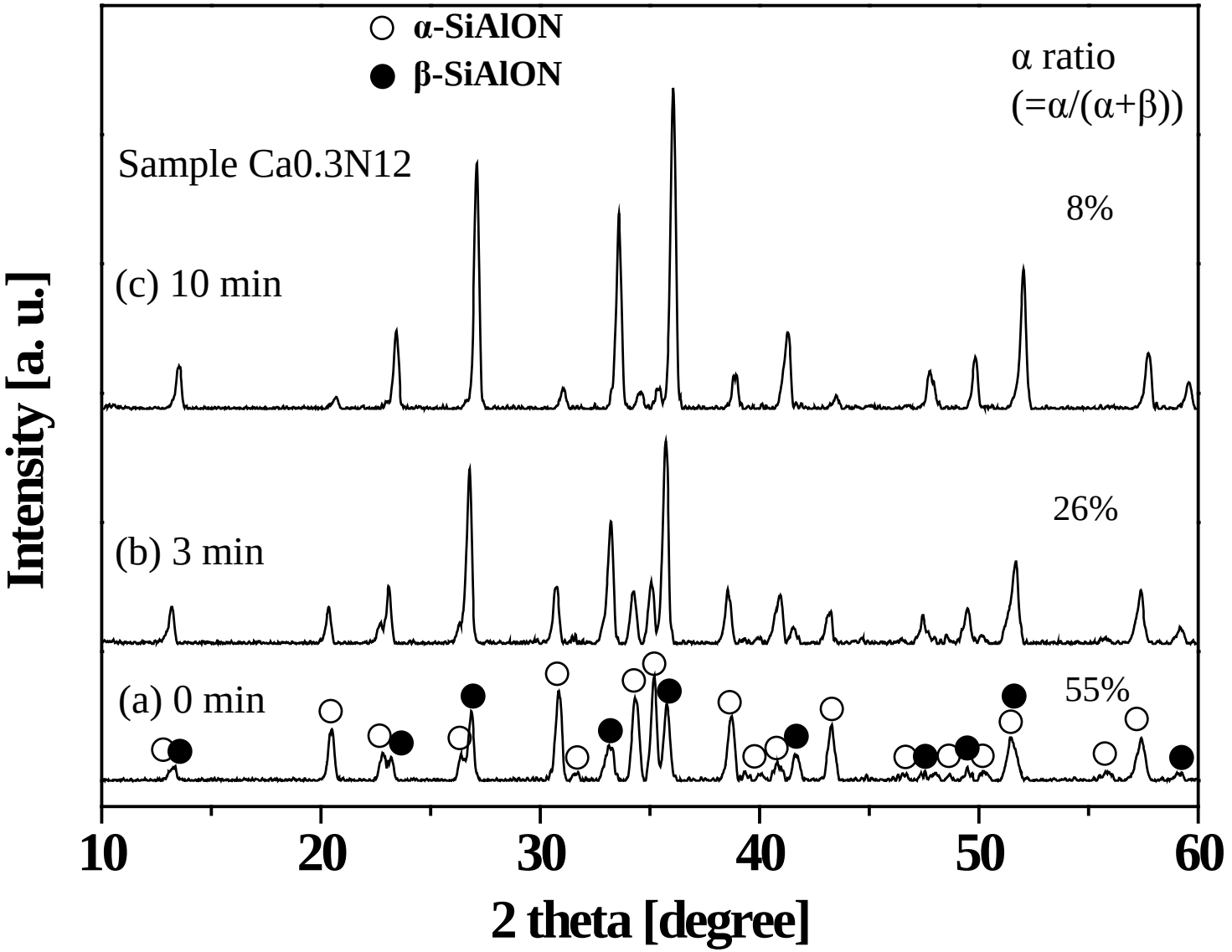

Fig. 5 XRD patterns of Ca0.3N12 sintered at 1600 ºC for: (a) 0 min: no holding, (b) 3 min and (c) 10 min.

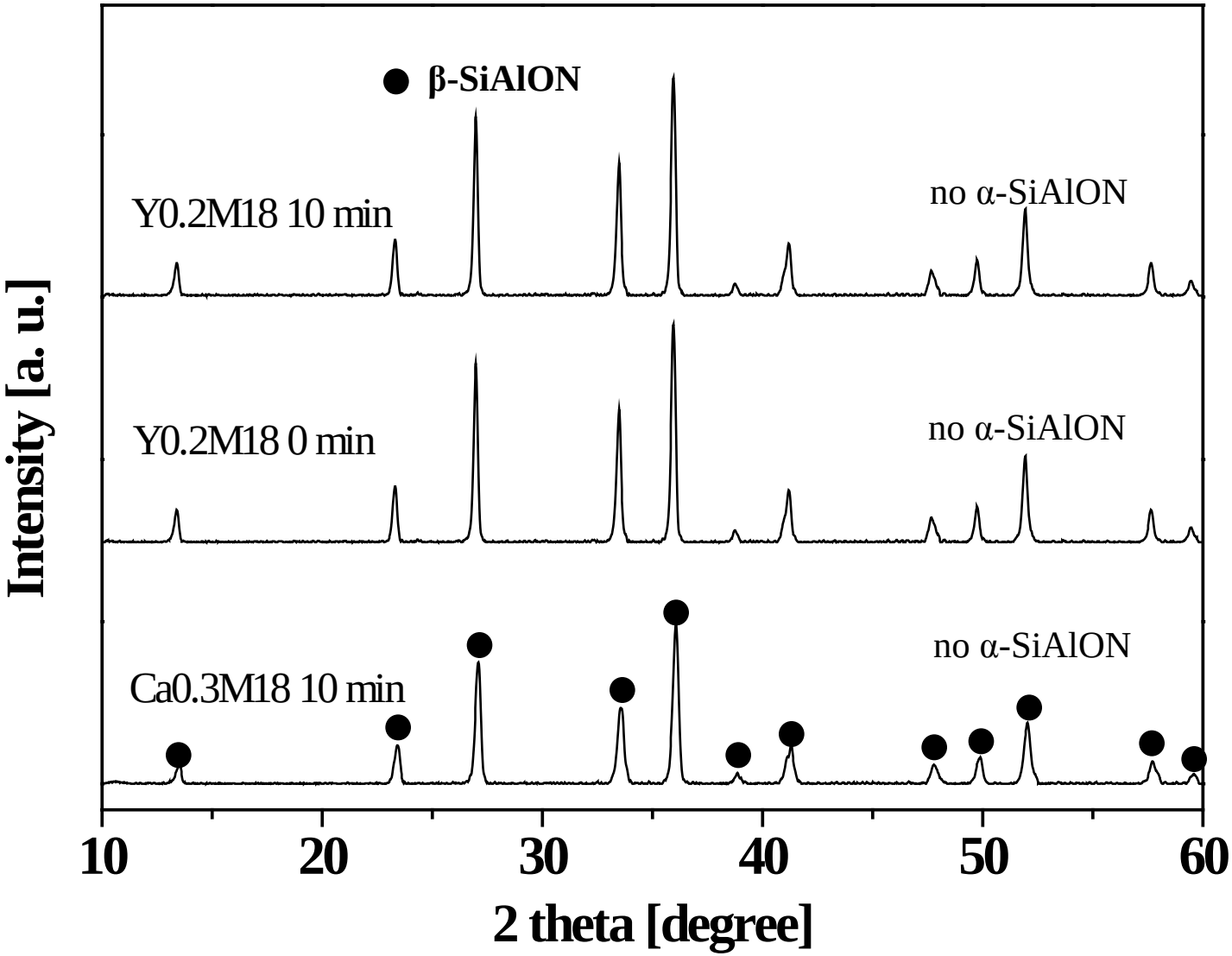

Fig. 6 XRD patterns of Y0.2M18 and Ca0.3M18 sintered at 1600 ºC with different holding times.

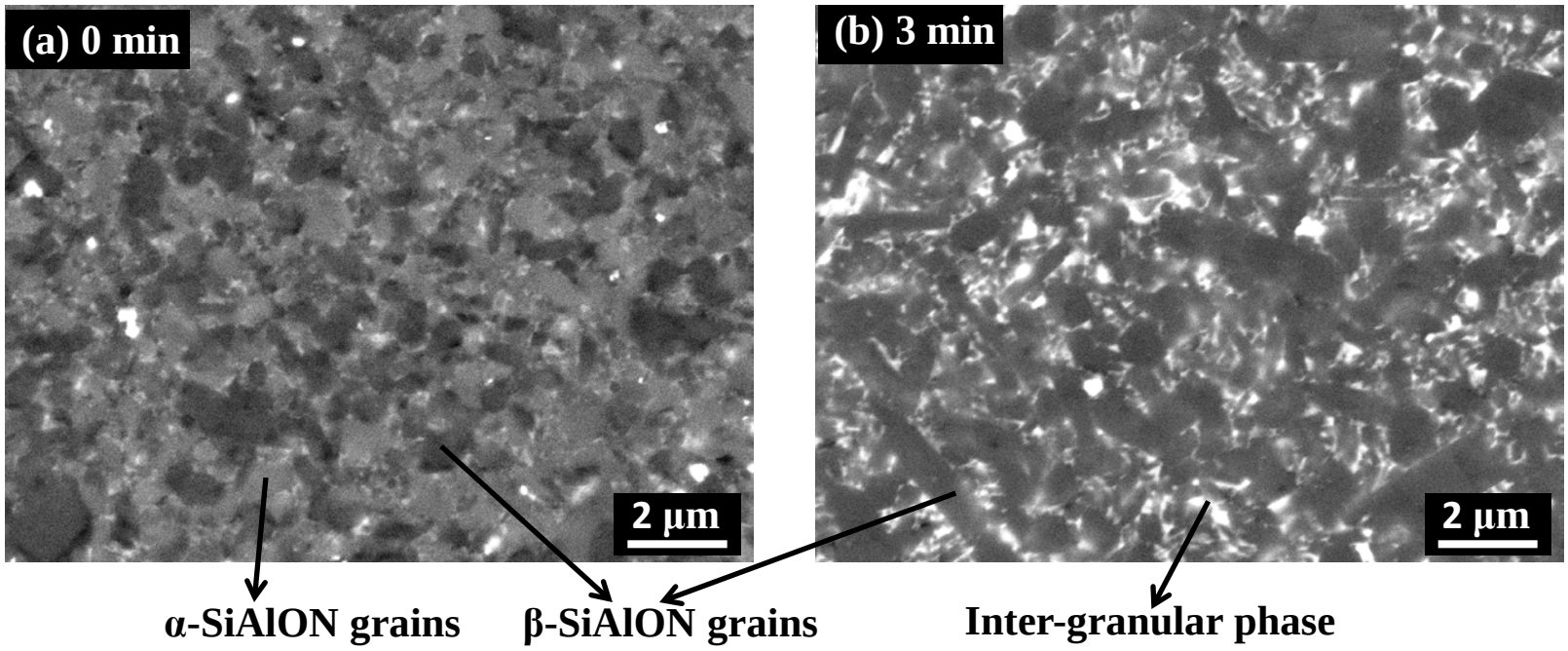

Fig. 7 Back-scattered micrographs of Y0.2N12 sintered at 1600 ˚C for: (a) 0 min: no holding and (b) 3 min. α-SiAlON, β-SiAlON, and glass phases are identified by grey, black and white contrast, respectively.

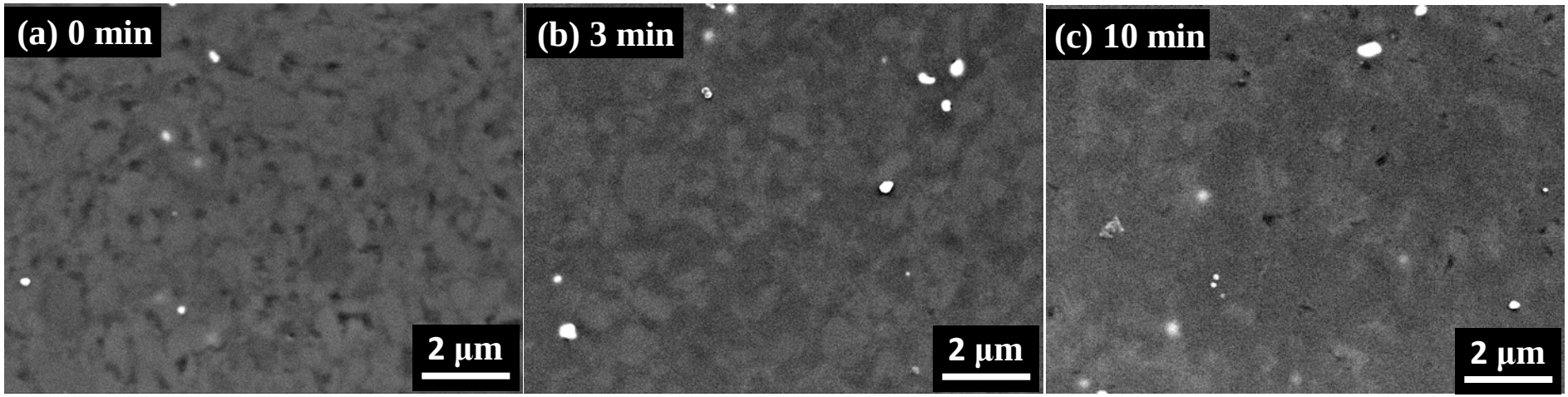

Fig. 8 Back-scattered micrographs of Ca0.3N12 sintered at 1600 °C for: (a) 0 min: no holding, (b) 3 min and (c) 10 min.